Clays and Clay Minerals, Vol. 37, No. 5, 396–402, 1989.

PREPARATION AND CHARACTERIZATION OF Al-RICH Zn-Al HYDROTALCITE-LIKE COMPOUNDS

F. THEVENOT, R. SZYMANSKI, AND P. CHAUMETTE

Institut Français du Pétrole, 1 & 4 Avenue de Bois Préau, B.P. 311
92506 Rueil-Malmaison Cedex, France

Abstract—Hydrotalcite-like compounds, described by the formula $[Zn_{1-x}Al_x(OH)_2][(CO_3)_{x/2}\cdot nH_2O]$, were prepared by coprecipitation methods at 80°C and characterized by bulk chemical analysis, X-ray powder diffraction (XRD), nuclear magnetic resonance (NMR), and scanning-transmission electron microscopy (STEM). An x value of 0.33 was previously assumed to be an upper limit, but recently, Al-rich hydrotalcite-like compounds have been prepared with x as large as 0.44 by hydrothermal synthesis. In the Zn-Al system, Al-rich hydrotalcite was synthesized at normal pressure by coprecipitation. Zn-Al hydrotalcite-like compounds were obtained in the range of $x = 0.3$ to 0.4. An Al-rich hydrotalcite-like compound with $x = 0.44$ was formed in mixtures containing large amounts of a poorly crystalline Zn-Al phase. A continuous contraction of the hydrotalcite-like structure occurred as x increased, both the a and c lattice parameters decreasing for x values as large as 0.44. This study illustrates the advantages of using quantitative analytical electron microscopy with high spatial resolution to complement conventional (and bulk) characterization techniques for correlating structural and compositional characteristics of finely divided materials.

Key Words—Hydrotalcite, Nuclear magnetic resonance, Scanning-transmission electron microscopy, Synthesis, X-ray powder diffraction, Zinc.

Résumé—Des composés de type hydrotalcite, de formule générale $[Zn_{1-x}Al_x(OH)_2][(CO_3)_{x/2}\cdot nH_2O]$, ont été préparés par coprécipitation, à 80°C, et caractérisés par différentes techniques telles que: analyse chimique globale, diffraction des rayons-X (DRX), résonance magnétique nucléaire (RMN), et microscopie électronique à transmission (STEM). Jusqu'à présent, la valeur de 0.33 était la limite supérieure admise pour x, mais récemment des phases de type hydrotalcite riches en Al ont été préparées, pour $x = 0.44$, par synthèse hydrothermale. Pour le système Zn-Al, nos résultats montrent que des composés de type hydrotalcite riches en Al peuvent être synthétisés à pression normale par coprécipitation. Des phases de type hydrotalcite à base de Zn et Al, ont été obtenues pour des valeurs de x comprises entre 0.3 et 0.4. Une phase hydrotalcite riche en Al avec $x = 0.44$ a été observée en mélange avec une grande quantité d'une phase à base de Zn et Al très mal cristallisée. Une contraction continue de la structure hydrotalcite est observée lorsque x augmente, les paramètres de maille a et c diminuent lorsque x augmente jusqu'à 0.44. Cette étude illustre les avantages de la microscopie électronique analytique à haute résolution spatiale, utilisée en complément des techniques de caractérisation conventionnelles, pour corréler les caractéristiques structurales et chimiques de matériaux finement divisés.

INTRODUCTION

Hydrotalcite-like compounds (HT) can be described by the general formula $[M^{2+}_{1-x}M^{3+}_x(OH)_2]^{x+}[X^{m-}_{x/m}\cdot nH_2O]$ where $M^{2+} = Mg^{2+}, Zn^{2+}, Ni^{2+}\ldots$, $M^{3+} = Al^{3+}, Fe^{3+}\ldots$, $X^{m-} = OH^-, Cl^-, NO_3^-, CO_3^{2-}\ldots$, and $0.25 \leq x \leq 0.33$ (Miyata, 1975; Gastuche *et al.*, 1967; Allmann, 1970). Serna *et al.* (1982) showed that the above formula should be extended to include some monovalent cations in the octahedral positions. These materials crystallize in either the $R\bar{3}m$ space group (rhombohedral phase) or the $P6/mmc$ space group (hexagonal phase). The a and c cell parameters of both phases depend, respectively, on the cations and anions present in the structure; the relationships between the cell parameters are $a_{hex} = a_{rh}$ and $c_{hex} = (2/3)c_{rh}$ (Allmann, 1968, 1970; Taylor, 1969, 1973). Generally, these HT structures are described as an alternation of positively charged brucite-like layers $[M^{2+}_{1-x}M^{3+}_x(OH)_2]^{x+}$ and negatively charged interlayers. In the rhombohedral phase three double-layers are present per unit cell: BC-CA-AB-BC and $c = 3c'$. In the hexagonal phase, two double-layers only are present per unit cell: BC-CB-BC and $c = 2c'$ (Allmann, 1970; Ingram and Taylor, 1967).

Synthetic HTs have found many industrial applications related to their anion-exchange properties (Reichle *et al.*, 1986; Sissoko *et al.*, 1985). Cu-, Co-, Zn-, and Al-based hydrotalcite-like hydroxycarbonates obtained by coprecipitation methods have been used by Institut Français du Pétrole (IFP) as precursors of mixed oxide catalysts for alcohol synthesis from syngas (Sugier and Freund, 1978, 1981).

Although a considerable amount of literature has been devoted to the properties of synthetic HTs containing divalent and trivalent cations, the relation between their structural and compositional characteristics is not clear. In minerals, the value of x in the HT formula ranges between 0.22 and 0.33. The value of 0.33 has been assumed to be the upper limit of x, even

in synthetic HTs, on the basis of crystal chemical considerations (Brindley and Kikkawa, 1979), because Al hydroxide formed in most syntheses from starting materials in which $x \geq 0.33$. Many patents claim the use of synthetic HTs having higher x values (e.g., *Miyata et al.,* 1975), but few details have been published. More recently Pausch *et al.* (1986) reported the hydrothermal synthesis of Al-rich HTs having $x = 0.44$ for the Mg-Al system. Here, however, the a lattice parameter of the HTs remained contant above $x = 0.33$, and the synthesis of Al-rich HTs was demonstrated on the basis of the bulk chemical analysis of their materials before and after washing in NaOH (to exclude the possibility of noncrystalline Al hydroxide phases). Thus, Al-rich HTs have apparently not been unambiguously identified.

Published syntheses illustrate a more general problem encountered in the study of finely divided synthetic powders or microprecipitates. To correlate precisely structural and compositional characteristics, very homogeneous phases must be obtained, especially if bulk methods of characterization are used, such as X-ray powder diffraction (XRD) and atomic absorption (AA). Unfortunately, minor impurity phases cannot always be avoided, and it may be impossible to wash out or even detect those that have formed. In many investigations of finely divided synthetic materials, the risk of not detecting or of neglecting secondary phases thought to be present in small amounts in the system must be accepted, or the study must be limited to only those phases that can be separated.

The use of quantitative analytical electron microscopy with high spatial resolution offers an opportunity to overcome such problems. At our laboratory a methodology has been developed that is based on the analysis by scanning-transmission electron microscopy (STEM) of thin foils of the solids obtained by ultramicrotomy, in conjunction with the other conventional techniques of characterization. This approach has been applied successfully to different types of finely divided materials in the field of heterogeneous catalysis (Lynch *et al.,* 1987; Szymanski *et al.,* 1987; Toulhoat *et al.,* 1987). In the present paper, the advantage of this approach is illustrated for investigating the synthesis of Al-rich HTs by coprecipitation methods in the Zn-Al system. In particular, the coprecipitation of Zn-Al HTs with $x \geq 0.33$ is demonstrated, and the a lattice parameter of the HTs is shown to decrease continuously up to $x = 0.44$ in this system.

EXPERIMENTAL

Materials synthesis

The basic hydrotalcite-like materials, $[Zn_{1-x}Al_x(OH)_2][(CO_3)_{x/2} \cdot nH_2O]$, were obtained by coprecipitation of a solution of 0.5 M Zn and Al nitrates in the suitable ratio (Zn/Al being varied between 3 and 0.5) with an aqueous solution of NaOH and Na_2CO_3. The concentration of NaOH was 0.2 M, and a proper amount of sodium carbonate was added to keep the ratio $CO_3^{2-}/(Zn + Al) \geq 1/8$. Temperature and pH were maintained at 80°C and 9, respectively. After coprecipitation, $NaOH/Na_2CO_3$ was added to increase the pH of the stirred mixed suspension to 10. The precipitate was then aged for an additional 15 min in the mother-liquor at pH 10 at 80°C. The precipitate was then filtered and washed thoroughly with distilled water at room temperature to remove the sodium ions, and finally dried for 16 hr at 40°C and for 3 hr at 90°C.

Physical characterization

Chemical analysis. The amounts of Al, Zn, and Na of each sample were determined by atomic absorption (AA) with a Perkin Elmer 5000 spectrometer. H, C, N, and O were determined by organic elemental analysis.

X-ray powder diffraction. The XRD powder pattern of each sample was obtained using a Philips PW1050 goniometer with CoKα radiation ($\lambda = 1.79$ Å). The lattice parameters of each hydrotalcite-like structure were determined using a least-squares cell-parameters refinement program (LSQ). This refinement was made from an XRD powder pattern collected with a quartz internal standard.

Nuclear magnetic resonance. ^{27}Al nuclear magnetic resonance (NMR) spectra were obtained with a Bruker CXP200 spectrometer using magic-angle spinning (MAS). $Al(H_2O)_6^{3+}$ was used as reference.

Electron microscopy. Samples were examined by scanning-transmission electron microscopy (STEM) using a dedicated VG HB5 instrument equipped with a Tracor TN5500/8500 energy-dispersive X-ray spectrometer (EDX) and image processor, a Gatan 607 electron-energy-loss spectrometer (EELS), and a high-sensitivity video camera for dynamic recording of electron microdiffraction patterns (ED). Thin foils of the solids, a few hundred of Ångstroms in thickness, were obtained by ultramicrotomy using a diamond knife on grains previously embedded in an epoxy resin. Quantitative information was obtained from the EDX spectra using a method based on the Cliff-Lorimer K-ratio approach (Szymanski and Lynch, 1986).

RESULTS

Six samples (A to F) were prepared having a bulk value of $x = Al/(Al + Zn)$ (determined by AA) ranging from 0.26 (A) to 0.65 (F). Bulk chemical analysis of samples A to F are listed in Table 1 along with the theoretical values calculated from the HT formula, $Zn_{1-x}Al_x(OH)_2(CO_3)_{x/2} \cdot nH_2O$, where n varies between 4 and 2 when x ranges from 0.26 to 0.65 (Allmann, 1970). The calculated atomic weight percentages were

https://doi.org/10.1346/CCMN.1989.0370502 Published online by Cambridge University Press

Table 1. Results of bulk chemical analyses (wt. %) of samples A, B, C, D, E, and F.[1]

Sample	x exp.	Zn		Al		C		O		H	
		Th.	Exp. ± 0.5	Th.	Exp. ± 0.5	Th.	Exp. ± 0.2	Th.	Exp. ± 0.5	Th.	Exp. ± 0.2
A	0.26	45.5	45.1	6.56	6.50	1.46	1.57	43.7	44.2	2.85	2.52
B	0.29	43.0	42.1	7.36	7.20	1.64	1.68	45.1	46.4	2.95	2.73
C	0.33	40.4	41.2	8.18	8.35	1.82	1.78	46.5	45.9	3.06	2.71
D	0.37	37.6	37.6	9.09	9.10	2.02	1.84	48.1	48.7	3.17	2.93
E	0.43	35.9	36.2	11.2	11.3	2.49	1.71	47.6	48.0	2.76	2.87
F	0.65	22.0	25.4	16.5	19.2	3.67	1.15	54.7	51.7	3.12	2.53

Th. = theoretical; Exp. = experimental.

[1] Theoretical atomic weight fractions were calculated from the formula $Zn_{1-x}Al_x(OH)_2(CO_3)_{x/2}\cdot nH_2O$.

close to the experimental values for all samples, except samples A, E, and F, for which larger discrepancies were observed. The low Na and N values for all precipitates, respectively <50 ppm and <0.05%, should be noted.

The XRD patterns of samples A to F showed sharp and symmetrical peaks characteristic of well-crystallized HTs and were indexed in rhombohedral symmetry, as illustrated in Figure 1 for sample C. Table 2 reports the relative intensities of the reflections, the observed and calculated d-values, and the a and c lattice parameters obtained from the LSQ refinement program for each sample. Small amounts of ZnO in samples A and B, and bayerite in sample E were detected. In sample F, the most Al-rich precipitate, broad XRD reflections were noted at about 4.7, 2.89, and 2.44 Å. These were attributed to the presence of an unidentified, poorly crystalline phase coprecipitated with the HT.

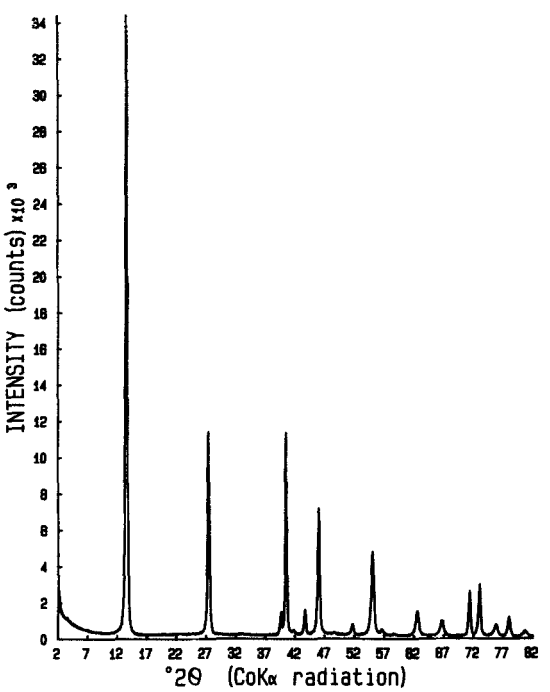

Figure 1. X-ray powder diffraction pattern of sample C (hydrotalcite-like phase).

^{27}Al NMR spectra of samples A to E showed a single resonance at +13 ppm (relative to $Al(H_2O)_6^{3+}$ reference) (Figure 2), corresponding to octahedral Al, characteristic of the HT structure (Reichle *et al.*, 1986; Schutz and Biloen, 1987). For sample F, the octahedral resonance was observed at +6 ppm. A weak resonance at about +50 ppm was also detected, corresponding to tetrahedral Al. These two resonances were attributed to the poorly crystalline phase detected by XRD.

These results demonstrate that Zn-Al HT was present in each sample and that a structural evolution occurred, inasmuch as both the a and c lattice parameters of the HT structure decreased from sample A to sample F. The correlation of a and c with the x value in the HT formula was, however, apparently limited to samples C and D, inasmuch as impurity phases were detected in samples A, B, E, and F. For samples B and E, their contribution may be neglected, because only weak peaks of ZnO and bayerite, respectively, were detected by XRD, and NMR and chemical analysis revealed no significant amounts of other noncrystalline phases (to the limit of experimental error). For samples A and F, in which all results confirmed the presence of ZnO and a large amount of a poorly crystalline, Al-containing phase, a microscopic approach was necessary to determine the x values of the respective HTs.

Observation by STEM showed in all samples the presence of well-crystallized hexagonal platelets, about 0.5 to 1 μm in size, yielding characteristic spotty ED patterns (Figure 3). This morphology is characteristic of the synthesized HT and was the only morphology observed in samples C, D, and E. The presence of ZnO was confirmed in sample A (Figure 4) and in sample B in lesser amounts. In sample F, large amounts of an additional phase were observed, formed by agglomerates of very small particles, showing diffuse-ring ED patterns, which corresponded to the poorly crystalline phase detected by XRD (Figure 5).

The use of EDX in the STEM allowed the compositional homogeneity in the individual HT platelets to be checked on a statistical population in each sample. The average x values obtained on the HT by EDX are

https://doi.org/10.1346/CCMN.1989.0370502 Published online by Cambridge University Press

Table 2. Observed and calculated X-ray powder diffraction data for synthetic hydrotalcite-like compounds (HT).

	A: $x = 0.26$			B: $x = 0.29$			C: $x = 0.33$			D: $x = 0.37$			E: $x = 0.43$			F: $x = 0.65$		
hkl	I/I_0	d obs.	d calc.	I/I_0	d obs.	d calc.	I/I_0	d obs.	d calc.	I/I_0	d obs.	d calc.	I/I_0	d obs.	d calc.	I/I_0	d obs.	d calc.
003	100.0	7.62	7.6167	100.0	7.63	7.6117	100.0	7.55	7.5483	100.0	7.52	7.5300	100.0	7.51	7.5313	100.0	7.48	7.5150
006	37.0	3.81	3.8083	36.9	3.81	3.8058	34.3	3.77	3.7742	38.2	3.76	3.7650	41.7	3.77	3.7657	44.7	3.76	3.7575
101	5.9	2.647	2.6491	6.5	2.645	2.6478	4.5	2.639	2.6423	3.6	2.635	2.6339	3.4	2.632	2.6316	7.9	2.624	2.6251
012	41.2	2.597	2.5973	42.1	2.595	2.5960	33.8	2.587	2.5899	30.0	2.581	2.5818	28.7	2.579	2.5796	37.9	2.572	2.5733
104	5.8	2.415	2.4167	6.3	2.413	2.4154	4.9	2.406	2.4078	4.3	2.401	2.4005	4.5	2.399	2.3988	10.5	2.394	2.3930
015	25.8	2.302	2.3035	26.4	2.301	2.3023	21.4	2.292	2.2939	20.9	2.287	2.2871	20.6	2.286	2.2857	32.7	2.280	2.2802
107	3.1	2.065	2.0654	3.4	2.063	2.0642	2.6	2.054	2.0548	2.3	2.049	2.0489	2.5	2.049	2.0480	6.1	2.043	2.0432
018	17.4	1.949	1.9494	18.3	1.947	1.9483	14.2	1.938	1.9386	14.9	1.933	1.9331	15.1	1.933	1.9323	22.2	1.928	1.9279
0012	—	—	1.9042	—	—	1.9029	1.7	1.888	1.8871	1.7	1.883	1.8825	2.1	1.884	1.8828	3.4	1.878	1.8788
1010	5.9	1.736	1.7353	6.1	1.734	1.7342	4.7	1.724	1.7244	4.8	1.720	1.7197	5.3	1.720	1.7192	8.4	1.715	1.7153
0111	4.3	1.639	1.6388	4.4	1.638	1.6379	3.2	1.628	1.6281	3.3	1.624	1.6237	3.4	1.624	1.6233	6.6	1.620	1.6197
110	9.2	1.5401	1.5399	10.5	1.5392	1.5391	7.7	1.5362	1.5360	6.2	1.5307	1.5312	5.0	1.5299	1.5298	8.5	1.5259	1.5260
113	9.7	1.5093	1.5093	11.1	1.5081	1.5086	8.7	1.5052	1.5052	7.0	1.5002	1.5004	6.0	1.4994	1.4991	10.0	1.4956	1.4955
1013	3.1	1.4688	1.4676	3.2	1.4670	1.4668	2.3	1.4572	1.4573	2.8	1.4530	1.4535	2.9	1.4530	1.4533	7.2	1.4508	1.4500
116	3.9	1.4278	1.4276	4.5	1.4268	1.4268	3.5	1.4230	1.4227	3.1	1.4180	1.4183	3.0	1.4173	1.4173	6.0	1.4142	1.4139
a ±0.001		3.0797 Å			3.078 Å			3.072 Å			3.062 Å			3.059 Å			3.052 Å	
c ±0.01		22.85 Å			22.83 Å			22.65 Å			22.59 Å			22.59 Å			22.54 Å	

d-values in Ångstroms.

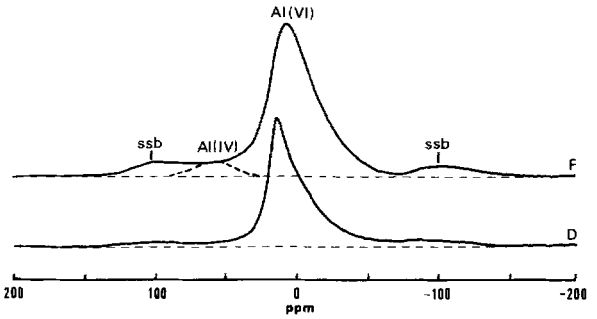

Figure 2. ^{27}Al nuclear magnetic resonance spectra of samples D (hydrotalcite-like compounds (HT)) and F (HT + poorly crystalline phase).

reported in Table 3, where they are compared with the bulk x values of the precipitates determined by AA. An estimation of the proportion of additional phase present in samples A and B (ZnO), E (bayerite), and F (poorly crystalline phase in which $x = 0.74$) is also indicated. The amount of impurity was calculated for each sample, by partitioning Zn and Al between the HT and the other phase for the given bulk composition.

The x values determined by EDX in STEM were close to the bulk x values for samples B, C, and D and

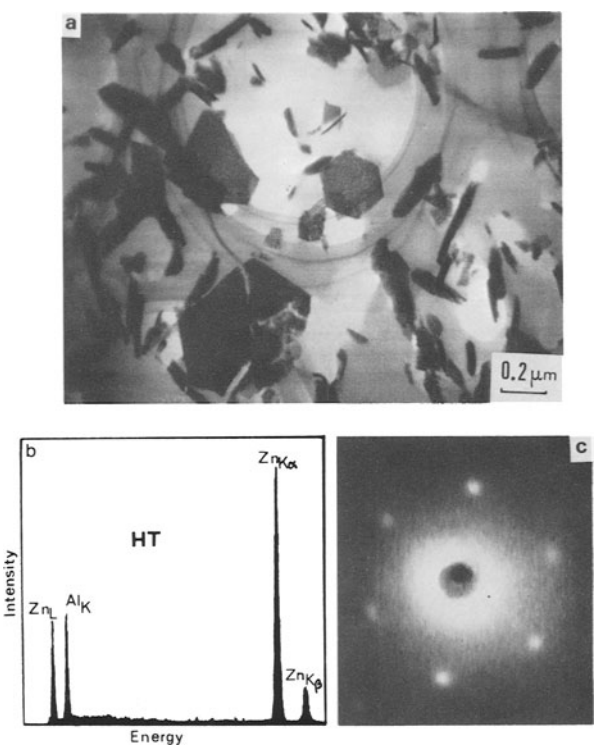

Figure 3. Characterization by scanning-transmission electron microscopy of the hydrotalcite-like compounds (HT) (example of sample C): (a) bright-field image showing the platelike morphology of HT; (b) energy-dispersive X-ray spectrum obtained on an individual HT platelet; (c) electron microdiffraction pattern of an individual HT platelet.

https://doi.org/10.1346/CCMN.1989.0370502 Published online by Cambridge University Press

Table 3. Scanning-transmission electron microscopy (STEM) and energy-dispersive X-ray (EDX) analysis of hydrotalcite-like phases (HT).[1]

Sample	x = Al/(Zn + Al) Bulk (AA)	HT platelets (EDX/STEM)	Additional phase (wt. %)
A	0.26	0.29 ± 0.02	ZnO (≃9%)
B	0.29	0.30 ± 0.02	ZnO (≃1%)
C	0.33	0.33 ± 0.02	
D	0.37	0.37 ± 0.02	
E	0.43	0.39 ± 0.02	bayerite (≃5%)
F	0.65	0.44 ± 0.02	poorly crystalline phase (≃65%) (x = 0.73)

[1] Nature and proportion of additional phases as determined by X-ray powder diffraction (XRD).

substantiated the overall homogeneity of these samples demonstrated by the other analytical techniques (ZnO was practically negligible in sample B). The data also confirmed the validity of the quantitative approach used in EDX, despite some problems of stability of the HT under the intense electron beam of the STEM. Beam damage, coupled with the intrinsic limitations of quantitative process, affected the precision on x (cf. Table 3). For samples A, E, and F, the amounts of additional phases were appreciable, and the x values determined for the HTs were significantly different from the bulk compositions. The x value of the HT in sample

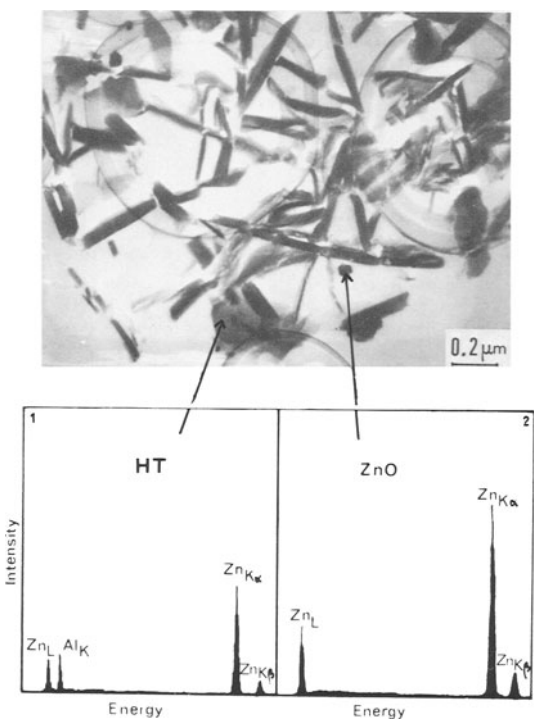

Figure 4. Scanning-transmission electon microscopy characterization of sample A (ZnO + hydrotalcite-like compound (HT)), showing energy-dispersive X-ray spectra for HT and ZnO.

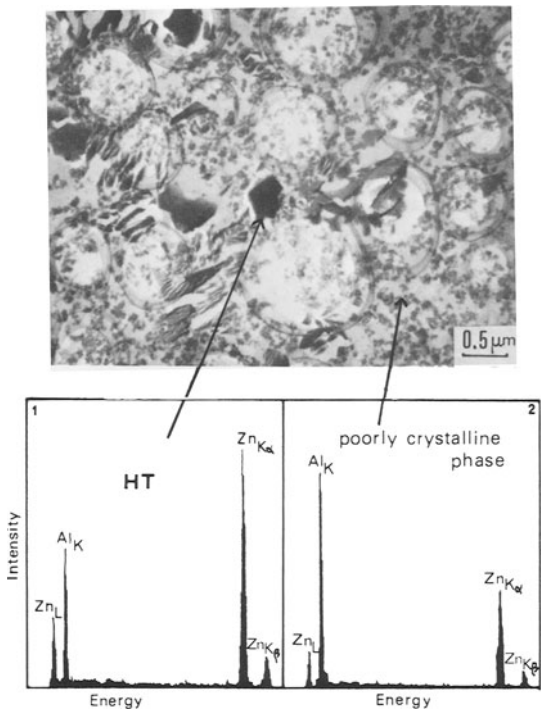

Figure 5. Scanning-transmission electron microscopy characterization of sample F (poorly crystalline phase + hydrotalcite-like compound (HT)).

A was close to that of sample B, which is consistent with the close structural characteristics of the HT in both samples. Note that for sample E, a value of x = 0.39 was found for the HT vs. 0.43 for the precipitate. This difference emphasizes the risk of significant errors if the contribution of Al hydroxide was neglected, as first proposed, on the basis of the bulk methods results. Finally, the data obtained for sample F fully illustrates the advantage of the microscopic analysis because, for this sample, it was the only method able to evaluate x in the HT. The value of 0.44 for the HT, vs. 0.65 for the overall precipitate, was the upper limit of x observed for the HT prepared in our precipitation conditions.

DISCUSSION AND CONCLUSIONS

Homogeneous Al-rich HT phases were synthesized in the range of x = 0.3 to 0.39 (samples B, C, D, and E). An HT phase with x = 0.44 was obtained, but only in a mixture with an unidentified poorly crystalline phase (sample F). These results confirm, for the Zn-Al system, the possibility of synthesizing Al-rich HT phases with $x > 0.33$ at normal pressure by coprecipitation methods. The upper value of x = 0.44 corresponds to that observed for Mg-Al-HT (Pausch *et al.*, 1986), probably a coincidence. Investigations are in progress to prepare HTs with still higher x values, perhaps in mixture with other phases.

https://doi.org/10.1346/CCMN.1989.0370502 Published online by Cambridge University Press

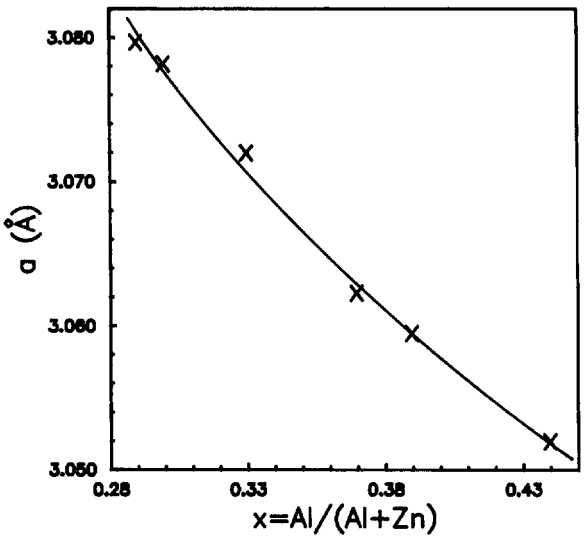

Figure 6. Variation of a lattice parameter as a function of x = Al/(Al + Zn) in the hydrotalcite-like structure (HT).

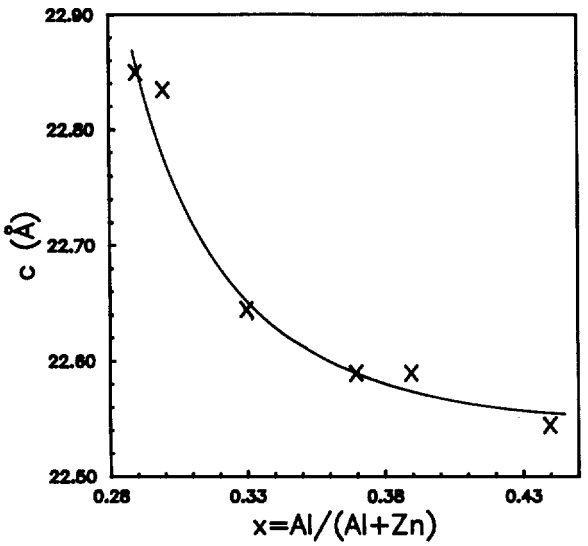

Figure 7. Variation of c lattice parameter as a function of x = Al/(Al + Zn) in the hydrotalcite-like structure (HT).

As shown in Figures 6 and 7, the a and c lattice parameters decreased continuously as a function of the x value of the HTs from samples A to F. As x increased from 0.3 to 0.44, a decreased from 3.08 to 3.05 Å and c, from 22.85 to 22.54 Å. Such variation is consistent with a compression of the HT structure, as described in other studies. The c parameter has been shown to depend on the thickness of the octahedral sheet, the thickness of the anion sheet, and the strength of the electrostatic attraction between the different sheets, whereas the a parameter has been shown to depend mainly on the size of the octahedral cation (cf. ionic radii) (Brindley and Kikkawa, 1979; Brown, 1980). Accordingly, a larger x value, i.e., a more substitution of Zn by Al, which increases the electrostatic attractive force between the brucite-like sheets and the anion interlayers, leads to a decrease in the c parameter. The resulting lowering of the mean weighted radius of the octahedral cations upon substitution leads to a decrease in the a parameter.

As proposed in previous studies (Brindley and Kikkawa, 1979), the variation of the a lattice parameter can be correlated with x by considering in a first approximation that in an ideal octahedral layer, $a = \sqrt{2}\cdot$ (M–O), where M–O is the metal ion-oxygen distance. The mean metal-ion radius for the present samples is $\bar{r} = (1 - x)r(Zn) + xr(Al) = r(Zn) - x(r(Zn) - r(Al))$, and the slope of the curve $a = f(x)$ is $\Delta a/\Delta x = -\sqrt{2}[r(Zn) - r(Al)]$. In the linear part of the experimental curve (Figure 6), i.e., in the region of $x \simeq 0.3$–0.35, the slope is about -0.23, which is in agreement with the value of -0.29 calculated from the above formula (using the ionic radii, r(Zn) = 0.74 Å and r(Al) = 0.53 Å). For larger x values, i.e., for greater Zn^{2+} substitution by Al^{3+}, electrostatic repulsion within the octahedral layer increases because of the greater amount of Al^{3+}. These electrostatic repulsion effects are likely to affect this simple linear relationship between a and x, and an attenuation of the decrease of a could occur for $x \geq 0.44$, as observed for the c parameter for $x \geq 0.35$ (Figure 7). Such an attenuation seems to have been observed for Mg-Al HT, for which the a value was found to remain constant at 3.04 Å for $x \geq 0.33$ (Pausch *et al.*, 1986). The continuous decrease of a, observed up to $x = 0.44$ in Zn-Al HT, does not contradict these results, because, for the present study, the value of a = 3.07 Å at $x = 0.33$, instead of 3.04 Å for Mg-Al HT, due to the larger ionic radius of Zn compared with Mg, and decreases to 3.05 Å at $x = 0.44$. New syntheses should permit verification of the occurrence of such attenuation effects on a.

Finally, this investigation clearly illustrates the advantages of using quantitative analytical electron microscopy with high spatial resolution in conjunction with other analytical techniques to characterize finely divided materials. Such an approach could be extended to most studies of microprecipitates to provide a better understanding of their chemistry and structure.

REFERENCES

Allmann, R. (1968) The crystal structure of pyroaurite: *Acta Crystallogr.* **B24,** 972–977.

Allmann, R. (1970) Doppelschichtstrukturen mit brucitähnlichen Schichtionen $[Me^{II}_{1-x}Me^{III}_{x}(OH)_2]^{x+}$: *Chimia* **24,** 99–108.

Allmann, R. and Jepsen, H. P. (1969) Die Struktur des Hydrotalkits: *Neues Jahrb. Mineral. Monatsh.* **12,** 544–551.

Allmann, R. and Lohse, H.-H. (1966) Die Kristallstruktur des Sjögrenits und eines Umwandlungsproduktes des Koenenits (= Chlor-Manasseits): *Neues Jahrb. Mineral. Monatsh.* **6,** 161–180.

Brindley, G. W. and Kikkawa, S. (1979) A crystal-chemical

study of Mg,Al and Ni,Al hydroxy-perchlorates and hydroxy-carbonates: *Amer. Mineral.* **64,** 836–843.

Brown, G. (1980) Associated minerals: in *Crystal Structures of Clay Minerals and their X-ray Identification,* G. W. Brindley and G. Brown, eds., Mineralogical Society, London, 397–400.

Gastuche, M. C., Brown, G., and Mortland, M. M. (1967) Mixed magnesium-aluminium hydroxides: *Clay Miner.* **7,** 177–201.

Ingram, L. and Taylor, H. F. W. (1967) The crystal structures of sjörgrenite and pyroaurite: *Mineral. Mag.* **36,** 465–479.

Lynch, J., Raatz, F., and Dufresne, P. (1987) Characterization of the textural properties of dealuminated HY forms: *Zeolites* **7,** 333–340.

Miyata, S. (1975) The syntheses of hydrotalcite-like compounds and their structures and physico-chemical properties—I: The systems Mg^{2+}-Al^{3+}-NO_3^-, Mg^{2+}-Al^{3+}-Cl^-, Mg^{2+}-Al^{3+}-ClO_4^-, Ni^{2+}-Al^{3+}-Cl^-, and Zn^{2+}-Al^{3+}-Cl^-: *Clays & Clay Minerals* **23,** 369–375.

Miyata, S., Kumura, T., and Shimada, M. (1975) Composite metal hydroxides: *U.S. Patent* **3,879,523,** 72 pp.

Pausch, I., Lohse, H.-H., Schürmann, K., and Allmann, R. (1986) Syntheses of disordered and Al-rich hydrotalcite-like compounds: *Clays & Clay Minerals* **34,** 507–510.

Reichle, W. T., Kang, S. Y., and Everhardt, D. S. (1986) The nature of the thermal decomposition of a catalytically active anionic clay mineral: *J. Catalysis* **101,** 352–359.

Schutz, A. and Biloen, P. (1987) Interlamellar chemistry of hydrotalcites. I. Polymerisation of silicate anions: *J. Solid State Chem.* **68,** 360–368.

Serna, C. J., Rendon, J. L., and Iglesias, J. E. (1982) Crystal-chemical study of layered $[Al_2Li(OH)_6]^+X^- \cdot nH_2O$: *Clays & Clay Minerals* **30,** 180–184.

Sissoko, I., Iyagba, E. T., Sahai, R., and Biloen, P. (1985) Anion intercalation and exchange in $Al(OH)_3$-derived compounds: *J. Solid State Chem.* **60,** 283–288.

Sugier, A. and Freund, E. (1978) Process for manufacturing alcohols, particularly linear saturated primary alcohols from synthesis gas: *U.S. Patent* **4,122,110,** 8 pp.

Sugier, A. and Freund, E. (1981) Process for manufacturing alcohols and more particularly saturated linear primary alcohols from synthesis gas: *U.S. Patent* **4,291,126,** 8 pp.

Szymanski, R. and Lynch, J. (1986) Quantitative X-ray microanalysis of divided solids in the STEM: in *Proc. 11th Int. Conf. X-Ray Optics and Microanalysis,* J. D. Brown and R. H. Packwood, eds., University of Western Ontario Graphic Services, London, Canada, 412–415.

Szymanski, R., Travers, C., Chaumette, P., Courty, Ph., and Durand, D. (1987) Comparison of the quantitative studies by STEM of hydrated hydroxycarbonates and related mixed oxide catalysts for CO hydrogenation to alcohols: in *Preparation of Catalysts IV,* B. Delmon, P. Grange, P. A. Jacobs, and G. Poncelet, eds., Elsevier, Amsterdam, 739–751.

Taylor, H. F. W. (1969) Segregation and cation-ordering in sjögrenite and pyroaurite: *Mineral. Mag.* **37,** 338–342.

Taylor, H. F. W. (1973) Crystal structures of some double hydroxide minerals: *Mineral. Mag.* **39,** 377–389.

Toulhoat, H., Plumail, J. C., Houpert, Ch., Szymanski, R., Bourseau, P., and Muratat, G. (1987) Modeling RDM catalysts deactivation by metal sulfides deposits: An original approach supported by HREM investigations and pilot tests results: in *Symposium on Advances in Residue Upgrading, American Chemical Society, Denver, 1987, ACS Preprints* **32,** p. 463 (abstract).

(Received 27 August 1988; accepted 2 January 1989; Ms. 1819)